ACS Catalysis

pubs.acs.org/acscatalysis

Research Article

En Route to a Heterogeneous Catalytic Direct Peptide Bond Formation by Zr-Based Metal−Organic Framework Catalysts

Francisco de Azambuja,[‡] Alexandra Loosen,[‡] Dragan Conic,[‡] Maxime van den Besselaar, Jeremy N. Harvey, and Tatjana N. Parac-Vogt*

Cite This: *ACS Catal.* 2021, 11, 7647−7658

Read Online

ACCESS | Metrics & More | Article Recommendations | Supporting Information

ABSTRACT: Peptide bond formation is a challenging, environmentally and economically demanding transformation. Catalysis is key to circumvent current bottlenecks. To date, many homogeneous catalysts able to provide synthetically useful methods have been developed, while heterogeneous catalysts remain largely restricted to the studies addressing the prebiotic formation of peptides. Here, the catalytic activity of Zr_6-based metal−organic frameworks (Zr-MOFs) toward peptide bond formation is investigated using dipeptide cyclization as a model reaction. Unlike previous catalysts, Zr-MOFs largely tolerate water, and reactions are carried out under ambient conditions. Notably, the catalyst is recyclable and no additives to activate the COOH group are necessary, which are common limitations of previous methods. In addition, a broad reaction scope tolerates substrates with bulky and Lewis basic groups. The reaction mechanism was assessed by detailed mechanistic and computational studies and features a Lewis acid activation of carboxylate groups by Zr centers toward amine addition in which an alkoxy ligand on adjacent Zr sites assists in lowering the barrier of key proton transfers. The proposed concepts were also used to study the formation of intermolecular peptide bond formation. While intrinsic challenges associated with the catalyst structure and water removal limit a more general intermolecular reaction scope under current conditions, the results suggest that further design of Zr-MOF catalysts could render these materials broadly useful as heterogeneous catalysts for this challenging transformation.

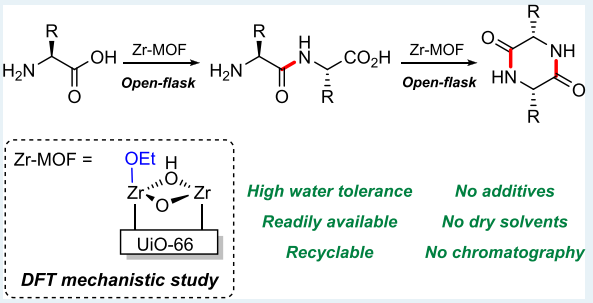

KEYWORDS: *metal−organic frameworks, synthesis, zirconium, amide bond, peptide bond, diketopiperazines, peptide synthesis, peptide bond formation*

INTRODUCTION

The synthesis of amides is a frequent task in every chemical laboratory. However, common procedures suitable to small laboratory scale fail to meet demanding industrial requirements.[1−3] Likewise, peptide bond formation is even more challenging due to the lower reactivity of the amino acid NH_2 group compared to regular amines.[4] In these reactions, carboxylic acids usually require additional steps and/or reagents to facilitate NH_2 attack, substantially decreasing process efficiency by increasing waste generation and energy consumption. Catalysis has been explored as an alternative to streamline amide synthesis, resulting in amide bond formations directly from nonactivated carboxylic acids and amines catalyzed mainly by boron[5] and group IV/V metal[6−9] catalysts.[10] Notably, catalytic peptide bond formation remains underdeveloped, despite advancements featuring boron-,[11−13] metal-,[14,15] and organocatalysts[16] reported recently. Although promising, these catalytic systems still require water removal from the reaction to provide good yields, making their reuse practically and economically challenging for wider industrial applications.[1,4] Recently, we have shown that embedding Zr(IV) or Hf(IV) cations into anionic oxo clusters imparts an unusual water tolerance to the catalytic reaction, allowing formation of amide bonds under mild conditions with great experimental simplicity and potential reuse of the catalyst.[17,18] Here, we extend this concept by using Zr(IV)-oxo clusters embedded in metal−organic frameworks (MOFs) as convenient and tailorable heterogeneous catalysts for peptide bond formation.

The synthesis of amides directly from nonactivated carboxylic acids and amines using heterogeneous catalysts is still of limited utility to synthetic chemists, despite numerous studies that have been done in the past.[10] Most reactions are limited to formylation and acylation reactions, with few examples reporting more general substrates.[19−22] Generally, these heterogenous catalysts afford amides under similar conditions to those used by homogeneous catalysts, that is,

Received: April 19, 2021
Revised: May 29, 2021
Published: June 10, 2021

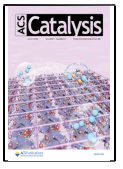

Table 1. Cyclization of GlyX (1a,b) to Cyclo(GlyX) (2a,b) Is Affected by the MOF Structure, Solvent, Temperature, and Catalyst Loading[a]

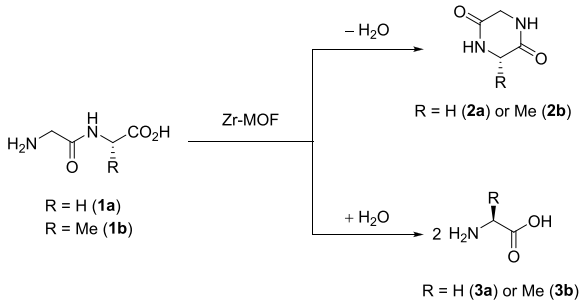

						yield (%)[b]		
entry	R	MOF	mol%	solvent	T (°C)	1a,b	2a,b	3a,b
1	H	MOF-808	10	DMSO	80	50	48	2
2	H	UiO-66	10	DMSO	80	65	33	0
3	H	MOF-808	10	MeOH	80	29	59	4
4	H	UiO-66	10	MeOH	80	0	100	0
5	Me	UiO-66	10	MeOH	80	0	100	0
6	Me	UiO-66	10	EtOH	80	0	100	0
7	Me	UiO-66	10	^{n}PrOH	80	0	100	0
8	Me	UiO-66	10	^{i}PrOH	80	n.a.[f]	58	0
9	Me	UiO-66	10	MeOH	70	8	92	0
10	Me	UiO-66	10	MeOH	60	35	65	0
11[c]	H	UiO-66	10	MeOH	80	0	100	0
12[d]	H	UiO-66	10	MeOH	80	6	94	0
13[e]	Me	UiO-66	2	MeOH	80	0	100	0

[a]Conditions: 0.100 mmol **1a,b**, 10.0 mol % MOF, solvent (0.10 mol L^{-1}), 24 h. [b]Based on ^{1}H-NMR. [c]0.05 mol L^{-1}. [d]0.20 mol L^{-1}. [e]168 h. [f]^{1}H NMR peaks of **1b** overlapped with solvent.

under (azeotropic) reflux at temperatures above 100 °C and anhydrous conditions. In addition, many of the heterogeneous catalysts reported so far consisted of commercially available inorganic oxides like Nb_2O_5, Al_2O_3, Zr_2O, TiO_2, SiO_2, etc., precluding control over the molecular environment surrounding the catalytic sites.[19,23−25] Attempts to rationally design inorganic matrixes doped with catalytically active metals have been done,[22] but despite recent advances in the areas of surface organometallic and single-atom catalysis,[26,27] tuning and designing heterogeneous catalysts at the molecular level remains a very challenging task, which limits to some extent the substrate scope expansion through a more rational design of novel catalysts. On the other hand, MOFs have emerged as a powerful new class of heterogeneous catalysts.[28−32] Strikingly different from other common heterogeneous materials, MOFs are intrinsically porous and highly tailorable organic−inorganic hybrid materials prepared through the controlled assembly of distinct metal clusters and specially designed organic linkers.[33] Moreover, an increasing number of methods allow engineering defects to fine-tune desired catalytic properties.[34−36] However, the use of MOFs in the amide bond formation remains elusive,[2,37] despite the successful reports of MOFs as catalysts in esterification reactions.[38−42] So far, only a single MOF-catalyzed amide bond formation has been reported focusing on the utility of a newly synthesized MOF material using previously reported conditions; however, this study provided little mechanistic insights that could allow further development of such chemistry.[43]

Recently, our work intersected with MOF catalysis due to our interest in developing heterogeneous artificial peptidases based on metal-oxo clusters.[44,45] To this end, we have pioneered the peptidase activity of Zr_6O_8-cluster-centered MOFs (Zr-MOFs) using MOF-808,[46,47] NU-1000,[48] and UiO-66[49] as catalysts. Among other practical advantages, these Zr-MOFs provided much higher hydrolysis rates than our previous Zr(IV)/Hf(IV)-polyoxometalate catalysts, prompting us to further evaluate if Zr-MOFs could also work in the reverse direction and lead to the formation of peptide bonds instead of its cleavage, as we observed previously for Zr(IV)/Hf(IV)-polyoxometalate complexes.[17] Prior works addressing the formation of peptide bonds through heterogeneous catalysis have been mostly related to the prebiotic formation of peptides.[50−54] They provided extensive mechanistic understanding on the interaction between amino acids and peptides with oxide surfaces, particularly silica, and the formation of peptide bonds in these environments.[55−57] The formation of peptide products has been generally observed at temperatures which exceeded 100 °C. Moreover, products were frequently generated as mixtures and were usually not isolated and purified, thereby drastically limiting the synthetic potential of these reactions for preparative organic chemistry.[58] Therefore, in view of the great structural versatility and stability of MOFs,[59,60] the increasing utility of Zr-MOFs in catalysis,[61] and the lack of more general heterogeneous catalysts for the catalytic direct formation of amide and peptide products,[10,19−22,43] repurpose of Zr-MOFs from hydrolysis to formation of peptide bonds would greatly contribute to develop a truly sustainable and practical peptide bond formation method. In this context, we report the formation of peptide bonds catalyzed by UiO-66 MOF. Inspired by our previous work,[17,46−49] we used dipeptide cyclization to develop and explore the catalytic activity of Zr-MOFs toward

https://doi.org/10.1021/acscatal.1c01782
ACS Catal. 2021, 11, 7647−7658

intramolecular peptide bond formation. Furthermore, we explored the reaction mechanism by theoretical and experimental approaches, which unveiled key advantages of the multimetallic nature of the Zr-oxo cluster to the reactivity observed. Initial results toward the intermolecular peptide bond formation reaction are also presented.

RESULTS AND DISCUSSION

Reaction Optimization. To develop Zr-MOFs as catalysts for the formation of peptide bonds, we have started our work by studying the cyclization of dipeptides in the presence of Zr-MOFs, following our previous successful strategy in which the hydrolytic activity of Zr(IV)/Hf(IV)-polyoxometalate complexes was repurposed to an amide bond formation reaction upon rational adjustment of the reaction conditions.[17,18] Thus, the cyclization of glycylglycine (**1a**) to 2,5-diketopiperazine (**2a**) was evaluated in various solvents upon incubation of **1a** with different Zr-MOFs, which were previously shown to be catalytically active for peptide bond hydrolysis (Table 1).[46,48,49] Based on our previous work,[17] we used DMSO as a representative organic solvent to test three well known and easily prepared Zr-MOFs with varying characteristics: (1) MOF-808, a 6-connected MOF with 1,3,5-benzenetricarboxylate linkers;[62] (2) NU-1000, an 8-connected MOF with 1,3,6,8-(*p*-benzoate)pyrene linkers;[63] and (3) UiO-66, a nominally 12-connected MOF with 1,4-benzenedicarboxylate (BDC) linkers.[64] The presence of free carboxylic acid groups in our substrate could result in adsorption of substrates or the resulting products onto the MOF catalyst. Therefore, we have employed a "washing step" after the reaction to ensure full material recovery. Using MOF-808 as a representative structure, we observed that stirring the crude reaction mixture for 1 h with D_2O generally ensured a high recovery of material (>95%). We have standardized such step through all the reaction discovery and optimization stages (Table S1).

In these initial reactions using DMSO as solvent, MOF-808 and UiO-66 provided **2a** in higher yields than NU-1000 (Figures S4 and S5), likely due to the lower recovery of material observed for NU-1000 (<20%). MOF-808 formed **2a** in ∼50% yield, but a small fraction of glycine (Gly, **3a**) was also detected probably arising from peptide bond hydrolysis with residual water present in the MOF structure and/or solvent (Table 1).[46] On the other hand, despite the lower yield, UiO-66 cleanly converted **1a** into **2a** (33% yield). Considering that MOF-808 and UiO-66 MOF allowed for an easier recovery of substrates and products in our system, further investigation focused on these MOFs only.

Following the initial screening, other solvents were probed using MOF-808 and UiO-66, identifying alcohols as optimal reaction solvents. Generally, MOF-808 adsorbed substrates and products more strongly than UiO-66, as observed by the mass recovery <75% for solvents other than MeOH and DMSO for MOF-808. For UiO-66, only MeCN:H_2O, toluene, and dioxane reactions resulted in <90% mass recovery for the ones carried out in an organic medium (Figures S4 and S5). Moreover, MOF-808 showed again a greater tendency than UiO-66 to hydrolyze **1a**, as evident from the results in solvents containing water. On the other hand, UiO-66's enhanced selectivity toward **2a** was once more observed for the reaction in MeOH, which provided only desired product **2a** and no hydrolysis side reaction (entry 4, Table 1). To test other alcohols, we used GlyAla (**1b**) instead of GlyGly (**1a**) to avoid overlap between product and solvent peaks in ^{1}H NMR. The minimal structural changes do not affect reactivity as both substrates smoothly provide the desired cyclic adduct **2a**,**b** in >99% in MeOH. Using **1b**, ethanol and 1-propanol also provided **2b** in >99% yield, while isopropanol resulted in only ∼60% yield, suggesting that smaller and linear alcohols are preferred as reaction solvents (entries 5−8, Table 1), though overlapped signals in crude ^{1}H NMR hampered us form establishing whether the lower yield in isopropanol is derived from lower conversion or simply from the lower mass recovery in this reaction.

In general, the low mass recovery observed in some cases seems to be related to the available uncoordinated Zr sites, and the ability of the solvent to reverse the binding of substrates and products to these sites, since lower mass recovery was generally observed for MOF-808 and NU-1000 in comparison with UiO-66. Similarly, lower mass recovery was also observed when cyclization was carried out in solvents that poorly solubilize **1a**,**b**/**2a**,**b** (e.g., dioxane and toluene for UiO-66). These trends strongly suggest that the interplay between the available Zr sites and the ability of the solvent to reverse the presumed coordination of substrates and products to these sites plays a key role in the overall process efficiency. When more Zr sites are available, more substrate/product molecules bind to MOF, and if the solvent is not able to efficiently reverse this trend, a lower mass recovery is observed. Such hypothesis is also consistent with the better, but rather intriguing performance of UiO-66 for the cyclization of **1a**,**b** in comparison with MOF-808 and NU-1000 MOFs, which intrinsically have more uncoordinated Zr sites than UiO-66. Together, these results show that the connectivity and missing-linker defects alone do not guarantee higher reaction yield as commonly indicated in the literature, since the adsorption of substrates and products onto the MOF material and the ability of the solvent to reverse it directly affects the overall mass recovery after the reaction, subsequently impacting the reaction yield. Interestingly, use of water as a reaction solvent resulted in the lowest recoveries for MOF-808 and UiO-66, suggesting solubility is likely not the only factor involved in overcoming material adsorption.

Further optimization was performed by probing the effect of temperature, concentration, and catalyst loading for the reaction using UiO-66 in methanol. Lower temperature decreased the reaction efficiency. At 70 °C, **2b** yield slightly decreased, and it significantly dropped for temperatures of 60 °C or lower (entries 9−10, Table 1 and Table S2). In addition, dilution or concentration of the reaction did not significantly affect efficiency (entries 11−12, Table 1 and Table S3). Finally, lower catalyst loadings also provided **2b** in quantitative yields, although slower rates were observed (Table S4). Using 2 mol % of UiO-66, **2b** was formed in 33% yield after 24 h. However, a longer reaction time of 168 h provided a quantitative yield, indicating that the catalyst is not deactivated by side processes even after considerably long reaction time (entries 13, Table 1). This robust profile is usual for Zr-MOFs but is unparalleled to other metal catalysts for the amide bond formation and further highlights the excellent catalytic potential of Zr-MOFs for peptide bond formation.

Control Experiments. Control experiments confirmed the superiority of UiO-66 as a heterogeneous catalyst for intramolecular peptide bond formation. In the absence of UiO-66, and when using Zr salts or BDC ligands separately, reaction yields were <10% (Table S5). Notably, soluble $Zr(^iPrO)_4$ and a combination of $ZrCl_4$ and BDC resulted in

https://doi.org/10.1021/acscatal.1c01782
ACS Catal. 2021, 11, 7647−7658

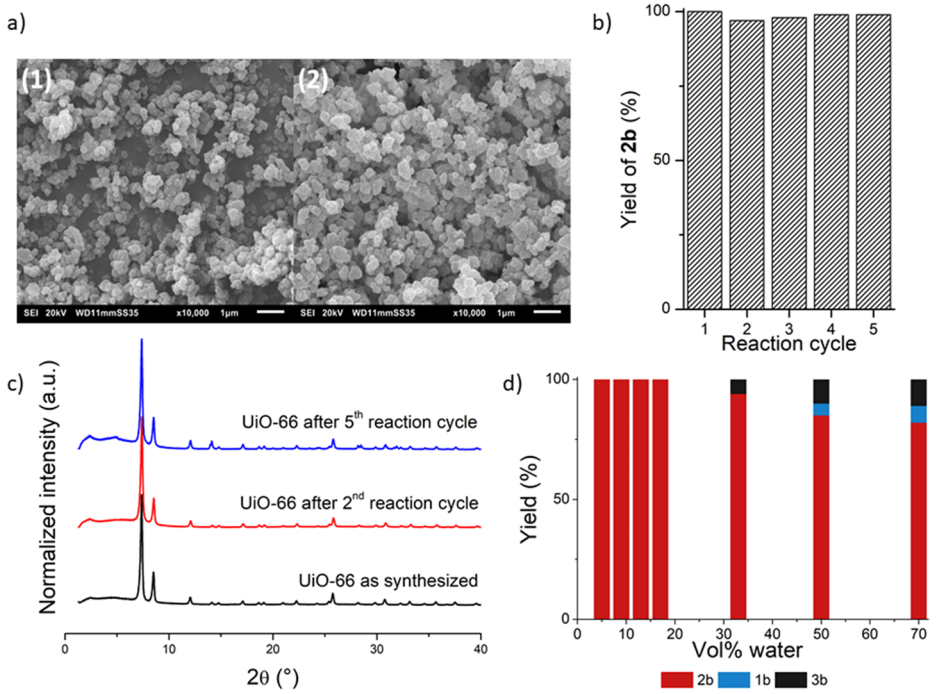

Figure 1. UiO-66 is a stable and recyclable catalyst with high tolerance toward water: (a) SEM images of (1) UiO-66 as synthesized and (2) after reaction with 0.100 mmol **1b**, 80 °C, 24 h, MeOH. (b) UiO-66 affords the same yields of **2b** after five reaction cycles. (c) PXRD pattern of UiO-66 as synthesized (black) and after two (red) and five (blue) reaction cycles with 0.100 mmol **1b**, 80 °C, 24 h and solvent exchange with D_2O and MeOH. (d) UiO-66 maintains its high catalytic performance even after addition of large amounts of external water.

good yields of **2b**, though lower than with UiO-66. The performance of $Zr(^iPrO)_4$ and $ZrCl_4$/BDC was attributed to a putative formation of Zr-oxo clusters in situ, which also points to the key catalytic role of UiO-66's Zr_6 clusters.[65,66] Additionally, control experiments using drying agents provided low yields of **2b**, strongly indicating that the water adsorption ability of MOF is likely not responsible for the observed reactivity (Table S5). Finally, the absence of reaction upon removal of the catalyst, along with UiO-66's stability observed in this work, strongly indicates that the catalysis is heterogeneous in nature (Figure S6).

Stability, Recyclability, and Water Tolerance of the UiO-66 Catalyst. Additional experiments confirmed the catalyst stability and prompted us to probe the UiO-66 recyclability and tolerance of the catalyst to water. UiO-66's excellent structural stability was confirmed through scanning electron microscopy (SEM) (Figure 1a), powder X-ray diffraction (PXRD), infrared spectroscopy (FT-IR), and thermal gravimetric analysis (TGA) of catalyst samples that were easily recovered by centrifugation from experiments with **1a,b** (Figures S7 and S9). Additionally, ICP-OES revealed very little leaching of Zr(IV) ions into solution (only 0.004%) confirming its structural stability and heterogeneous nature of the reaction. Furthermore, MOF digestion revealed ~5% of **1b** and **2b** after the reaction, indicating that minor amounts of the substrate and product remain adsorbed to the catalyst (Figures S11 and S12). This suggests non-negligible changes to the pore and surface of UiO-66 after the reaction and simple MeOH washing steps. Thus, recovered UiO-66 was washed with D_2O and MeOH to remove traces of the starting material and product before drying and reusing in a new reaction. This recycling protocol effectively afforded **2b** in >97% yield over five cycles (Figure 1b and Table S6), while no structural changes in MOF's crystalline network were detected by PXRD analysis (Figure 1c).

UiO-66 catalytic cyclization of **1b** tolerates uniquely large amounts of water, and >95% yield is observed in the presence of nearly 2800 molar excess of water with respect to the catalyst (Figure 1d and Table S7). UiO-66's stability prompted us to check its tolerance to the presence of water in the reaction, as water-sensitivity sharply limits large scale catalytic amide bond formations.[1,2,4] By adding increasing amounts of water to the standard reaction, >97% yield of **2b** was observed up until 27.8 mmol D_2O (33% of reaction volume in Figure 1d), which corresponds to a remarkable 2778-fold excess related to the catalyst (Table S7). Further reactions showed that this tolerance is related to the amount of MeOH, and lower yields were observed when the MeOH volume was reduced proportionally to the water added in order to keep the reaction concentration constant. However, even when water corresponded to 70% of the solvent, a respectable 82% yield of **2b** is still observed. Such results also strongly suggest the minor contribution of water segregating ability of MOF in driving the reaction equilibrium forward, in agreement with control experiments. A maximum water adsorption for UiO-66 of 0.55 g H_2O/g MOF has been reported,[67] which would mean that to adsorb the 70% water volume used in the referred reaction (~0.7 g), a much higher catalytic loading (~1.3 g of MOF, ~800 mol %) than the one used here (17 mg, 10 mol %) would be needed.

UiO-66 advantageous robustness in the presence of water was further confirmed by its better performance compared to other water-tolerant Lewis acid metal salts under the same conditions (Table S8).[68] When external water was added to the reaction catalyzed by $Zr(^iPrO)_4$ (20% of reaction volume), the good yield previously observed for **2b** in the aforementioned control experiments decreased by ~30%, which is

https://doi.org/10.1021/acscatal.1c01782
ACS Catal. 2021, 11, 7647−7658

consistent with general sensitivity of Zr(IV) salts to moisture, given their highly favored hydrolysis to form oligomeric catalytically inactive species.[10,69] However, PXRD analysis of UiO-66 after the reaction conducted in the presence of 50% v/v of water proved the stability of its overall structure under these conditions (Figure S13), demonstrating an intrinsic advantage of the Zr-based MOFs' robustness over conventional Zr catalysts based on metal salts or complexes thereof. In addition, other Lewis acids that have been reported to tolerate water were also tested in the presence and in the absence of water (Table S8). Even for these simple reactions, a general drop of 20−30% of yield was observed, with the best performing $Sc(OTf)_3$ providing **2b** in 80% of yield in the presence of 33% volume of water, while UiO-66 affords **2b** in 97% of yield under the same conditions. Considering the higher natural abundance of zirconium compared to the other Lewis acid metal salts tested (Ti excluded) and the recyclability exhibited by UiO-66 these results underline a promising prospect of Zr-MOFs, even when one contrasts the complexity of these materials with simple, commercially available metal salts.

Reaction Scope. Several other substrates were successfully shown to undergo cyclization and could be isolated in good to excellent yields, showcasing that the UiO-66 MOF catalyst can be applied to substrates bearing diverse functional groups (Table 2), which is essential for later development of intermolecular peptide bond forming methods catalyzed by Zr-MOFs. Standard substrate **1b** and Gly-Phe (**1c**) afforded product **2b** and **2c** in high purity and excellent isolated yields after a simple centrifugation and evaporation of the supernatant. In addition, indole, imidazole, hydroxyl, and thioether groups in **1d,f,g,i,j** were tolerated and the corresponding products **2d,f,g,i,j** were isolated in 68 to >99% yield. The electrospray ionization-mass spectrometry (ESI-MS) and NMR analysis of reactions using Gly-Lys and Gly-Arg dipeptides suggested that these substrates could also undergo cyclization; however, we could not isolate and characterize the corresponding products with our current protocol. Nevertheless, these results point to an overall good compatibility with Lewis basic functional groups.

Some steric hindrance was also tolerated since Gly-Pro (**1e**), a secondary amine, and the bulky side chain of Gly-Leu (**1h**) afforded products **2e** and **2h** in 92 and >99%, respectively. Similar **2b** and **2e** yields were obtained when glycine was moved to the C-terminal position of the dipeptide substrate, while a significant drop was observed for Ser-Gly (**1f**) (45%), likely due to a nonproductive coordination of the hydroxyl moiety. Even Ala-Ala (**1i**), a dipeptide without a glycine residue, was cyclized to **2i** in 18 and 33% yield after 24 and 96 h, respectively. Unnatural amino acids **1l,m** were also successfully cyclized, showing that the proteogenic nature of the substrate is not required for observing the reactivity.

Our attempts to cyclize longer oligomers such as tri-, tetra-, and pentaglycine or unnatural amino acids with distinct carbon chain lengths (4, 6, and 7) under the same conditions were unfortunately not successful. For most cases, neither substrates or products were observed after reactions, suggesting that the substrates remained adsorbed to the catalyst, which is consistent with the significant adsorption of longer peptides (e.g., proteins) to metal-oxo clusters observed in our previous works.[44,48] In general, cyclized products also showed different affinities for the MOF catalyst, including extreme cases like Gly-Asp (**1n**) and Gly-Glu (**1o**) which even leads to partial loss of the crystallinity rather than cyclization (Figure S14). Thus, in some cases, additional washings of the catalyst to remove the products were necessary. However, although not fully optimized, our isolation protocol afforded the cyclized products in good to excellent purity, and no liquid−liquid extraction or chromatographic purification was necessary.

Table 2. Intramolecular Amide Bond Formation from Dipeptides and Other Amino Acid Substrates[a]

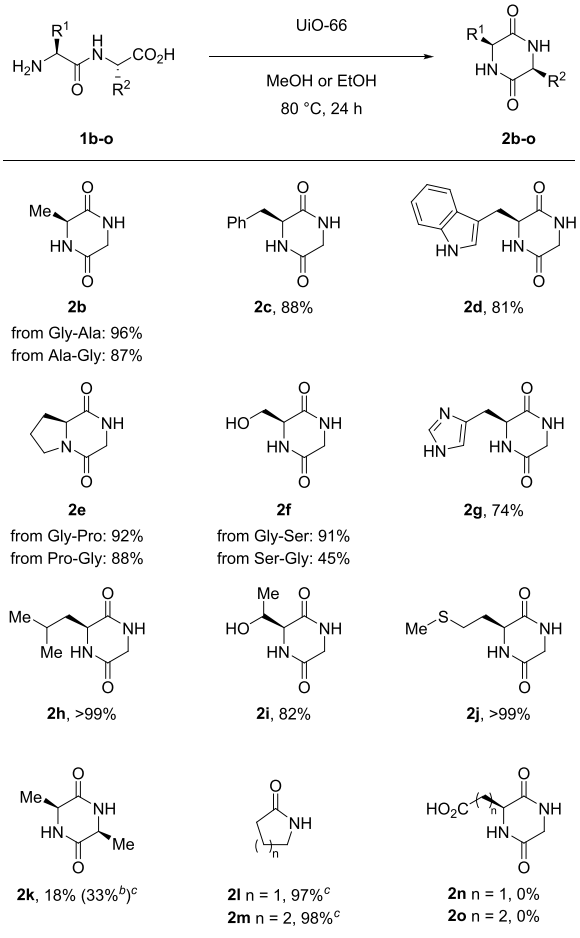

[a]Conditions: **1b-o** (0.100−0.500 mmol), 10.0 mol % UiO-66, MeOH or EtOH (0.10 mol L^{-1}), 80 °C, 24 h. Isolated yields. [b]96 h reaction. [c]^{1}H NMR yields.

Reaction Mechanism. To gain a better understanding of the catalyst activity, we carried out a detailed experimental and theoretical investigation of the reaction mechanism. Based on our own work,[46−49,70] previous reports on Zr-catalyzed formation of amides directly from nonactivated carboxylic acids and amines,[17,71] and control experiments reported here, we suggest a general Lewis acid catalytic pathway for this intramolecular amide bond formation in which the dipeptide carboxylate group is activated through coordination to an open Zr site of the MOF (Figure 2). However, the reasons for the superior reactivity observed in alcoholic solvents were not clear at the beginning since only the solvent influence in the mass recovery discussed above does not explain why the yield of **2a,b** in MeOH or EtOH is much higher when UiO-66 MOF is used as a catalyst in comparison to when MOF-808 is employed, given that >95% of the initial mass is recovered with both catalysts (Figures S4 and S5). Such observation prompted us to further investigate whether the alcoholic solvent plays an

https://doi.org/10.1021/acscatal.1c01782
ACS Catal. 2021, 11, 7647−7658

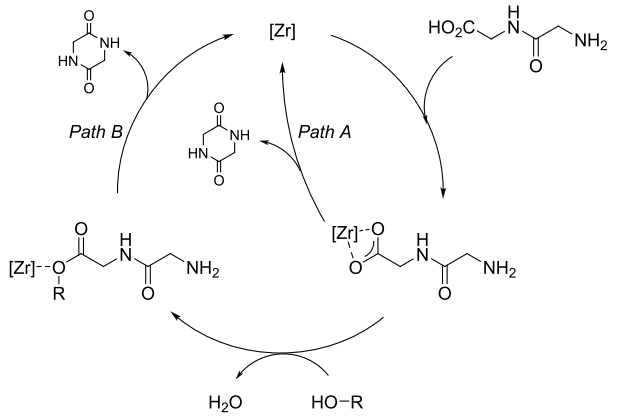

Figure 2. Mechanistic possibilities for the Zr-MOF-catalyzed intramolecular peptide bond formation.

additional role in the mechanism. Thus, we investigated whether both a superior proton transfer ability of alcoholic solvents inside the pores of UiO-66[72] or the formation of an intermediate ester[73] could explain the reactivity observed.

Reaction Kinetics. Different kinetic experiments were used to get a clearer picture of the catalyst activity, such as potential inhibition and involvement of intermediates. Substrate consumption directly leads to product formation judging by the mirrored aspect of the kinetic profile of **1b** cyclization, disfavoring a reaction pathway involving a potential intermediate product (Figure 3a). Using a pseudo-first-order kinetics model, a rate constant of 1.54×10^{-4} s^{-1} and a half-life of 1.2 h were obtained at 80 °C (Figure 3b). Upon increasing the temperature from 60 to 90 °C, a ≈17-fold reduction of the half-life from 16 h at 60 °C to only 0.9 h at 90

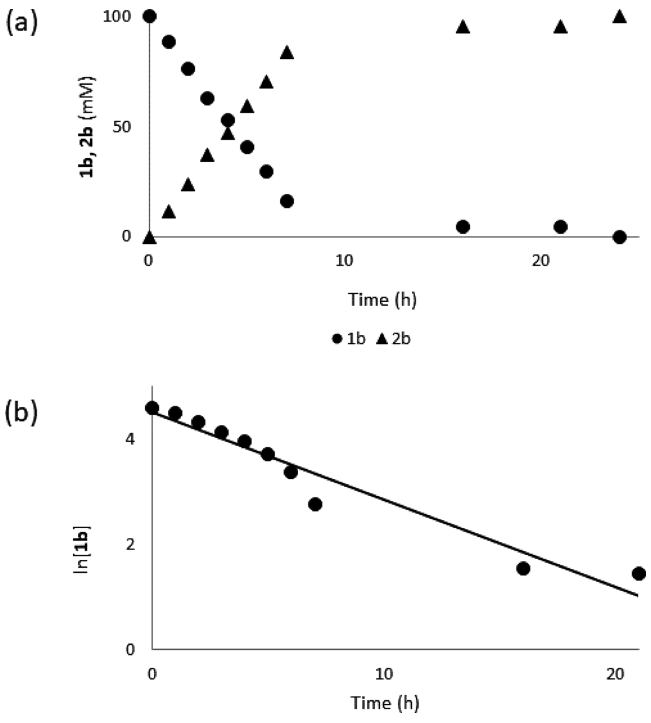

Figure 3. (a) Cyclization of GlyAla (**1b**, circles) to cyclo(GlyAla) (**2b**, triangles) as a function of time. (b) First-order decay fit of ln[**1b**] as a function of time. Conditions: 0.100 mmol **1b**, 10.0 mol % UiO-66, MeOH (0.10 mol L^{-1}), 80 °C. ^{1}H NMR yields.

°C was observed (Figure S15a). Fitting these data to the Eyring equation, we estimated $\Delta G^{\ddagger}$ = 27.2 kcal mol^{-1} at 80 °C ($\Delta H^{\ddagger}$ = 22.9 kcal mol^{-1}, $\Delta S^{\ddagger}$ = −12.1 cal mol^{-1} K^{-1}) (Figure S15b). Finally, control kinetic experiments in which the MOF is presaturated with product **2b** showed no difference in yield after 3 and 5 h in comparison with the noninhibited reaction, suggesting that no product inhibition happens (Table S10).

Potential Involvement of an Ester Intermediate. Motivated by the superiority of alcoholic solvents in our reactions, previous reports on the UiO-66 MOF-catalyzed esterification reactions under similar conditions,[40] the formation of peptide bonds from ester substrates,[74,75] and the facile cyclization of dipeptide esters to diketopiperazine products,[73] we have probed the potential involvement of an intermediate ester in the reaction mechanism as depicted in Figure 2. To check whether intermediate formation of an ester and subsequent cyclization to the final products **1a,b** could account for the superior reactivity observed in alcoholic solvents, we used GlyGly-OMe as a reaction substrate. After 3 h, GlyGly-OMe afforded **2a** in 89% yield (Table S11), showing the feasibility of a potential intermediate ester cyclization. When the cyclization was blocked by protection of the **1a** N-terminal position with an acetyl group, the ester was formed in ∼80% of yield after 24 h, indicating that ester formation may happen under these conditions (Table S12). However, little GlyGly-OMe (∼5%) was detected through ^{1}H NMR and ESI-MS when the reaction of **1a** was stopped before completion (Figure S16), suggesting that if ester is involved, its cyclization is likely not the rate-determining step.

Computational Study. Density functional theory (DFT) computations were also used to examine the mechanism of Zr-MOF-catalyzed dipeptide cyclization, focusing on modeling of the reaction in ethanol solvent, given the identical results for reactions involving EtOH and MeOH. Experimental characterization of the UiO-66 structure revealed our system to be similar to previous reports (see the Supporting Information (SI) for details); thus, we based our computational model on a previous computational work on UiO-66.[76,77] In this model, a representative cluster model of the MOF catalyst was chosen, comprising a single Zr_6 core unit with one BDC linker defect and an ethoxy group as a defect-capping ligand (see the SI for full computational details). Glycylglycine (**1a**) in its most stable canonical form in EtOH was used as a model substrate (Table S14).

At first, we compared the relative stability of different complexes formed from **1a** and the Zr_6 cluster, suggesting that the most stable form **A** involves **1a** coordinating to a Zr center through its carboxylate group in a monodentate fashion (Figure 4 and Figure S17). In **A**, the carboxylic acid group in **1a** is deprotonated and there is a neutral ethanol ligand at an adjacent Zr site. In general, other structures involving **1a** monodentate binding to the free Zr site were found to be lower in energy for the deprotonated dipeptide than for its neutral form. In these complexes, the relative energy was found to vary as a function of the nature of the anchoring group within **1a** that coordinates to the metal, in the order carboxylate group (most stable) < amide oxygen atom < NH_2 group.

Using structure **A** as a reactant complex, we considered two potential reaction pathways, namely, the formation of cyclic product **2a** through a direct cyclization of **1a** (*Path A*) or through the formation of an intermediate ester which cyclizes in situ (*Path B*) (Figure 2). The results suggest that an ester

https://doi.org/10.1021/acscatal.1c01782
ACS Catal. 2021, 11, 7647−7658

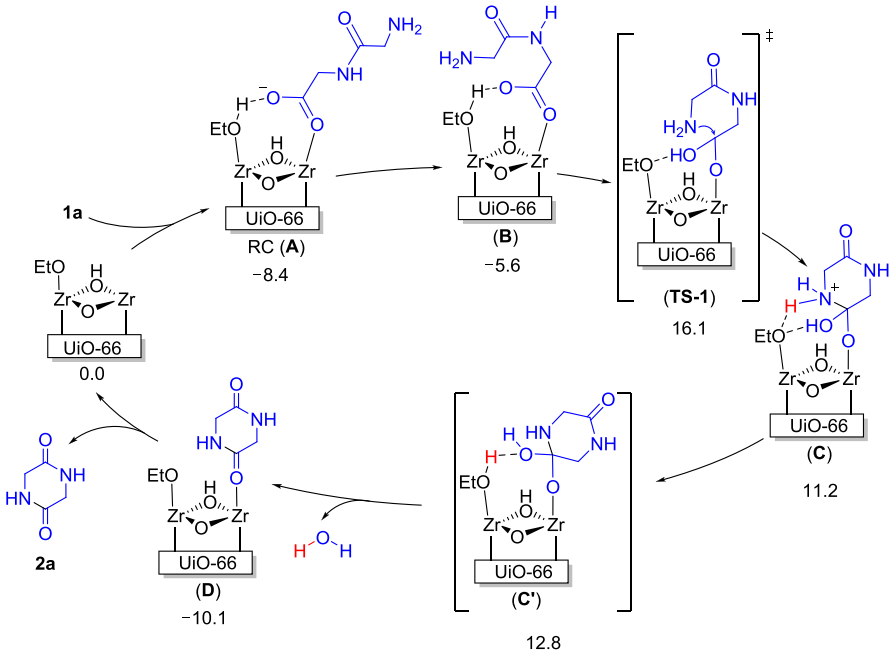

Figure 4. Intramolecular peptide bond formation reaction: SMD-B3LYP-GD3BJ/BS2 relative free energies (353.15 K, kcal mol^{-1}) for key intermediates and transition states along the computed reaction path (BS2 is a modified def2-TZVP basis set described in the SI).

intermediate is not involved since the calculated barrier for its formation lies at ∼30 kcal mol^{-1} above complex **A**, which is ca. 6 kcal mol^{-1} higher than the barrier for direct cyclization. This is consistent with our experimental observations that the ester is present in small amounts but can be formed in appreciable amounts if the cyclization is blocked through protection of the dipeptide's NH_2 group. Therefore, the reaction most likely proceeds through direct cyclization of **1a** (*Path A*).

Proposed Catalytic Cycle. Considering the DFT results, which are in line with experiments, a reaction mechanism is proposed in Figure 4 (Figure S18). From complex **A**, sequential peptide bond *trans*/*cis* isomerization, NH_2 attack, and water release steps take place to give the cyclized product **2a** (Figure 4). The *trans*/*cis* isomerization transition state (TS) features a pyramidal sp^3 geometry of the amide nitrogen atom,[78−80] which was computed to lie 23.1 kcal mol^{-1} above the reactant complex (**A**), and is consistent with an experimental $\Delta G^{\ddagger}$ of 20.9 kcal mol^{-1} for amide isomerization under similar conditions.[81] Moreover, our computed *trans*/*cis* ΔG = 2.8 kcal mol^{-1} matches the experimental value of 3.1 kcal mol^{-1}.[81] Next, the *cis*-isomerized intermediate **B** undergoes several low-barrier conformational changes that allow the NH_2 group to move closer to the carboxylate group in preparation for the rate-determining nucleophilic addition, which generates the cyclic tetrahedral intermediate **C**. The TS for nucleophilic addition is predicted to lie 24.5 kcal mol^{-1} above **A**, in good agreement with the experimentally derived $\Delta G^{\ddagger}$ of 27.2 kcal mol^{-1} (Figure 2 and Table S9). The 2.6 kcal mol^{-1} discrepancy is well within the estimated error bar of the protocol used here. In the last step, the cyclic intermediate **C** releases water through a low-barrier proton shift from the NH_2 to OH group of the tetrahedral carbon. This transfer is assisted by the adjacent ethoxy group, whose absence would otherwise require formation of a highly strained four-membered ring or the entropically disfavored involvement of an extra solvent molecule, resulting in higher energy barriers.[82] Next, the formed water molecule is released, ultimately resulting in separate products, which are characterized by ΔG = −14.2 kcal mol^{-1} relative to the separate reactants (see the SI for details).

Intermolecular Peptide Bond Formation. The many benefits of Zr-MOF catalysis for peptide bond formation outlined above prompted us to investigate whether intermolecular formation of peptide bonds could be achieved, as the MOF structure could favor the formation of this challenging amide bond.[83] Accordingly, glycine (**3a**) and UiO-66 were incubated in MeOH at 80 °C (Table 3). After 24 h, 20% of glycine was quantitatively converted into a **1a**:**2a** mixture (∼10:1 ratio) (Table 3, entry 1). Using longer reaction times increased the yield, reaching an encouraging 75% yield of a **1a**:**2a** (1:2.6 ratio) mixture after 168 h (Table 3, entry 3). Increasing the temperature to 100 °C improved the 24 h reaction combined yield to only 50%, and more of the cyclized product was observed (Table 3, entry 4). This sluggish

Table 3. Intermolecular Peptide Bond Formation[a]

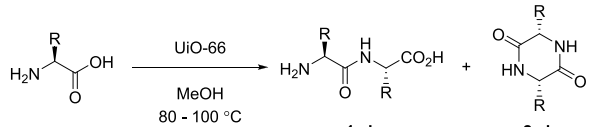

entry	R	T (°C)	mol. sieves?	time (h)	conversion (%)	yield 1 + 2 (%)	1:2
1	H	80		24	20	20	10:1
2	H	80		96	39	39	1.2:1
3	H	80		168	75	75	1:2.6
4	H	100		24	50	50	1:1.1
5[b]	H	100		24	50	50	1:1.3
6	H	100	yes	48	63	63	1:7
7	Me	100	yes	48	45	0	N.D.

[a]Conditions: **3a** (0.200 mmol), 10.0 mol % UiO-66, MeOH (0.10 mol L^{-1}), 80 °C, molecular sieves 3 Å (100 mg). ^{1}H NMR yields. [b]Dry MeOH.

https://doi.org/10.1021/acscatal.1c01782
ACS Catal. 2021, 11, 7647−7658

reactivity prompted us to consider the removal of water from the system, as it is well known that the equilibrium can be driven to the peptide bond formation through water scavenging.[84] However, using dry MeOH did not improve the yield (Table 3, entry 5), and combining dry MeOH with molecular sieves only improved the yield by 13% after 48 h (Table 3, entry 6). The apparent limited effect of molecular sieves in these reactions is puzzling and contradicts the generally observed trend with many other catalysts reported in the literature.[37] This could be related to the ability of Zr-MOFs to adsorb water,[67] thereby acting both as a desiccant and a catalyst; however, this potential dual effect of the MOF structure in the intermolecular reaction would require further studies in order to be confirmed. Notably, negligible reactivity was observed with $Zr(^{i}PrO)_4$ under standard conditions (80 °C, no molecular sieves), and only 46% of **1a**/**2a** combined was produced under dry conditions (100 °C, with molecular sieves) after 48 h. Furthermore, no products were observed without MOF in the presence or absence of molecular sieves. Together, these results evidence the beneficial effect of the MOF network in enhancing the reactivity (Table S16).[75]

The counterintuitive selectivity favoring **1** at shorter reaction times motivated us to investigate the mechanism of this reaction by DFT modeling of the key intermediates and transition states along the reaction path, as shown in Figure 4 (see the SI for more details). Our calculations estimated the energy barrier for the intermolecular reaction to be ∼4 kcal mol^{-1} higher relative to the "**3a**-free" intramolecular peptide bond formation, which is in qualitative agreement with the longer reaction times and selectivity observed for intermolecular reactions (Table 3 versus Tables 1 and 2), as well as the nonobservation of triglycine or longer oligomers. However, the observed **1a**:**2a** ratios obtained at early stages of the reaction together with similar binding energies of glycine and **1a** to UiO-66 suggest that **3a** might inhibit the cyclization (Figure 5). This inhibition was confirmed by adding **3a** to a standard GlyAla (**1b**) cyclization (17% yield vs 100% yield in the absence of **3a**, Table S18).

Attempts to extend the intermolecular reaction to other amino acids was not successful. A dimerization of alanine under the same conditions used for glycine failed to provide desired adducts (Table 3, entry 7). Attempts to optimize reaction concentration, temperature, and the presence or absence of molecular sieves were unfortunately not fruitful. In several cases, part of the initial alanine was not recovered, which was attributed primarily to its adsorption. However, aromatic signals coherent with a para-substituted aromatic ring could be detected in the NMR of crude reaction mixtures, suggesting that the MOF linker reacts preferably with the amino acid substrates bulkier than glycine. Though we were not able to identify the product formed, loss of the MOF network structure due to esterification of linkers has been reported before.[85] However, PXRD analysis after the reaction showed that the overall structure of MOF remains intact, suggesting that the lack of reactivity could not be due to MOF decomposition. Further attempts to facilitate the intermolecular peptide coupling led us to react H-Gly-OMe with different amino acids. However, in these reactions only **2a** was observed, and dimerization of H-Ala-OMe also did not afford the linear or cyclic product (Table S17).

This unexpected lack of reactivity with other amino acids led us to probe more conventional organic substrates such as phenylacetic acid and benzylamine under the same conditions

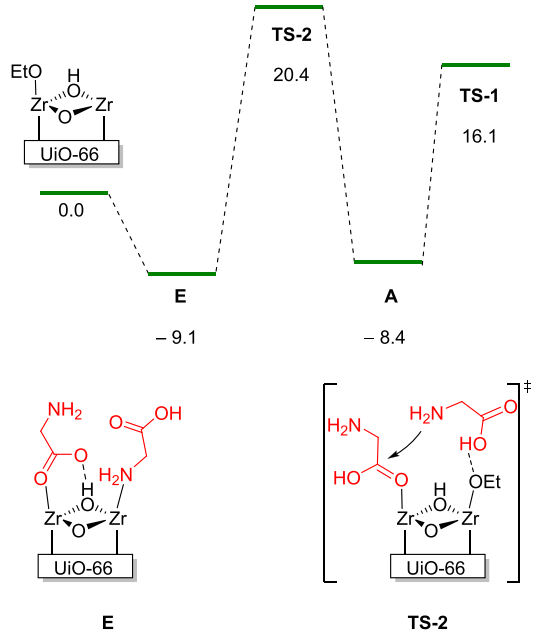

Figure 5. Intermolecular peptide bond formation reaction: SMD-B3LYP-GD3BJ/BS2 relative free energies (353.15 K, kcal mol^{-1}) for key intermediates and transition states along the computed reaction path (BS2 is a modified def2-TZVP basis set described in the SI).

(Table 4). The *N*-benzyl-2-phenylacetamide **6** product was observed in low yields even in the presence of molecular sieves

Table 4. UiO-66 Catalyzes Intermolecular Amide Bond Formation[a]

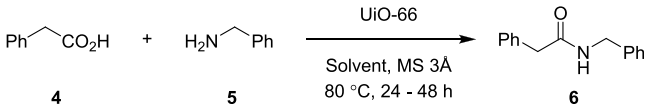

4 5 6

entry	solvent	mol. sieves?	time (h)	yield **6** (%)
1	EtOH	no	24	14
2[b]	EtOH	yes	24	18
3	1,4-dioxane	no	24	39
4	1,4-dioxane	no	71	41
5	1,4-dioxane	yes	71	88
6[b]	1,4-dioxane	yes	24	84 (75[c])
7[b,d]	1,4-dioxane	yes	24	16

[a]Conditions: **4** (0.100 mmol), **5** (0.150 mmol) 10.0 mol % UiO-66, molecular sieves 3 Å (50 mg), solvent (0.10 mol L^{-1}), 80 °C. ^{1}H NMR yields. [b]3 equiv of **5**. [c]Isolated yield. [d]No UiO-66 MOF.

(entries 1 and 2). Preliminary optimization could elevate the yield up to 88% by exchanging the reaction solvent to dioxane and using molecular sieves, whose effect in this case is in line with prior reports (entries 3−6).[6,86−88] These results show that the extent to which water removal affects the reaction depends on the substrate and/or reaction condition being used, and that even currently available Zr-MOFs might need water removal techniques to provide good yields after all. However, given that **6** was formed, the lack of reactivity observed with amino acids other than glycine suggests that it is rather the catalyst structure, and not the reaction itself or a poor water removal, that is precluding product formation. In this sense, the overall optimization of the Zr-MOF structure would be

https://doi.org/10.1021/acscatal.1c01782
ACS Catal. 2021, 11, 7647−7658

needed in order to make the catalytic activity more general toward intermolecular reactions.

Overall, these explorative results for the direct dimerization of unprotected commercially available amino acids showcases the potential of Zr-MOFs in streamlining the intermolecular catalytic peptide bond formation, although further optimization of the MOF catalyst structure is clearly necessary to expand the reaction scope to a broader range of amino acids.

CONCLUSIONS

In conclusion, we discovered the high potential of Zr-MOFs as a new class of heterogeneous catalysts for peptide bond formation. We have shown that UiO-66 efficiently catalyzes the intramolecular formation of peptide bonds directly from free amines and nonactivated carboxylic acids without any additives, drying agents, inert atmosphere, or special protocols to remove water from the reaction. Good yields were obtained for a variety of substrates containing Lewis basic functional groups and bulky side chains, including a secondary amine group. Remarkably, UiO-66 is stable under the reaction conditions and shows a water tolerance that largely superseded other Zr(IV) catalysts, resulting in a straightforward recycling of the catalyst and showcasing the potential of Zr-MOFs as viable sustainable and water-tolerant catalysts for amide bond formation. In addition, our detailed mechanistic investigation uncovered several important features for the design of future catalysts, such as (1) the interplay between the MOF structure, reaction solvent, and easy recovery of substrates and products, which might have a significant impact on the overall process efficiency, (2) the key role of an alkoxy group on the adjacent metal center in lowering the barrier of key proton transfers, and (3) the noninvolvement of an ester intermediate, indicating that a more general reaction scope is feasible for Zr-MOFs. Finally, we provide a proof of concept that a similar mechanism also enables the formation of intermolecular peptide bonds directly from unprotected commercially available glycine. Even though further catalyst structure optimization is needed to expand this reactivity to other amino acid precursors, these results underline a high catalytic potential of Zr-MOFs that can impact a broad range of scientific areas.

ASSOCIATED CONTENT

Supporting Information

The Supporting Information is available free of charge at https://pubs.acs.org/doi/10.1021/acscatal.1c01782.

Experimental procedures, supplementary experiments, copy of NMR spectra, computational study details, results, and cartesian coordinates (PDF)

AUTHOR INFORMATION

Corresponding Author

Tatjana N. Parac-Vogt − *Department of Chemistry, KU Leuven, 3001 Leuven, Belgium;* orcid.org/0000-0002-6188-3957; Email: tatjana.vogt@kuleuven.be

Authors

Francisco de Azambuja − *Department of Chemistry, KU Leuven, 3001 Leuven, Belgium;* orcid.org/0000-0002-5537-5411

Alexandra Loosen − *Department of Chemistry, KU Leuven, 3001 Leuven, Belgium;* orcid.org/0000-0001-5324-6483

Dragan Conic − *Department of Chemistry, KU Leuven, 3001 Leuven, Belgium;* orcid.org/0000-0002-6251-7254

Maxime van den Besselaar − *Department of Chemistry, KU Leuven, 3001 Leuven, Belgium*

Jeremy N. Harvey − *Department of Chemistry, KU Leuven, 3001 Leuven, Belgium;* orcid.org/0000-0002-1728-1596

Complete contact information is available at: https://pubs.acs.org/10.1021/acscatal.1c01782

Author Contributions

‡F. d. A., A. L., and D. C. contributed equally to this work.

Notes

The authors declare no competing financial interest.

ACKNOWLEDGMENTS

We thank KU Leuven and Research Foundation Flanders (FWO) for financial support. F.d.A. (195931/1281921N) and A.L. (48730/1S10318N) thank the FWO for fellowships.

REFERENCES

(1) Sabatini, M. T.; Boulton, L. T.; Sneddon, H. F.; Sheppard, T. D. A Green Chemistry Perspective on Catalytic Amide Bond Formation. *Nat. Catal.* **2019**, *2*, 10−17.

(2) Wang, X. Challenges and Outlook for Catalytic Direct Amidation Reactions. *Nat. Catal.* **2019**, *2*, 98−102.

(3) Dunetz, J. R.; Magano, J.; Weisenburger, G. A. Large-Scale Applications of Amide Coupling Reagents for the Synthesis of Pharmaceuticals. *Org. Process Res. Dev.* **2016**, *20*, 140−177.

(4) Isidro-Llobet, A.; Kenworthy, M. N.; Mukherjee, S.; Kopach, M. E.; Wegner, K.; Gallou, F.; Smith, A. G.; Roschangar, F. Sustainability Challenges in Peptide Synthesis and Purification: From R&D to Production. *J. Org. Chem.* **2019**, *84*, 4615−4628.

(5) Sabatini, M. T.; Karaluka, V.; Lanigan, R. M.; Boulton, L. T.; Badland, M.; Sheppard, T. D. Protecting-Group-Free Amidation of Amino Acids using Lewis Acid Catalysts. *Chem. − Eur. J.* **2018**, *24*, 7033−7043.

(6) Lundberg, H.; Adolfsson, H. Hafnium-Catalyzed Direct Amide Formation at Room Temperature. *ACS Catal.* **2015**, *5*, 3271−3277.

(7) Tsuji, H.; Yamamoto, H. Hydroxy-Directed Amidation of Carboxylic Acid Esters Using a Tantalum Alkoxide Catalyst. *J. Am. Chem. Soc.* **2016**, *138*, 14218−14221.

(8) Li, N.; Wang, L.; Zhang, L.; Zhao, W.; Qiao, J.; Xu, X.; Liang, Z. Air-stable Bis(pentamethylcyclopentadienyl) Zirconium Perfluorooctanesulfonate as an Efficient and Recyclable Catalyst for the Synthesis of N-substituted Amides. *ChemCatChem* **2018**, *10*, 3532−3538.

(9) Lundberg, H.; Tinnis, F.; Adolfsson, H. Zirconium catalyzed amide formation without water scavenging. *Appl. Organomet. Chem.* **2019**, *33*, No. e5062.

(10) Lundberg, H.; Tinnis, F.; Selander, N.; Adolfsson, H. Catalytic Amide Formation from Non-Activated Carboxylic Acids and Amines. *Chem. Soc. Rev.* **2014**, *43*, 2714−2742.

(11) Noda, H.; Furutachi, M.; Asada, Y.; Shibasaki, M.; Kumagai, N. Unique Physicochemical and Catalytic Properties Dictated by the B_3NO_2 Ring System. *Nat. Chem.* **2017**, *9*, 571.

(12) Sabatini, M. T.; Boulton, L. T.; Sheppard, T. D. Borate Esters: Simple Catalysts for the Sustainable Synthesis of Complex Amides. *Sci. Adv.* **2017**, *3*, No. e1701028.

(13) Michigami, K.; Sakaguchi, T.; Takemoto, Y. Catalytic Dehydrative Peptide Synthesis with gem-Diboronic Acids. *ACS Catal.* **2020**, *10*, 683−688.

(14) Muramatsu, W.; Tsuji, H.; Yamamoto, H. Catalytic Peptide Synthesis: Amidation of N-Hydroxyimino Esters. *ACS Catal.* **2018**, *8*, 2181−2187.

(15) Muramatsu, W.; Yamamoto, H. Tantalum-Catalyzed Amidation of Amino Acid Homologues. *J. Am. Chem. Soc.* **2019**, *141*, 18926−18931.

(16) Handoko; Satishkumar, S.; Panigrahi, N. R.; Arora, P. S. Rational Design of an Organocatalyst for Peptide Bond Formation. *J. Am. Chem. Soc.* **2019**, *141*, 15977−15985.
(17) de Azambuja, F.; Parac-Vogt, T. N. Water-Tolerant and Atom Economical Amide Bond Formation by Metal-Substituted Polyoxometalate Catalysts. *ACS Catal.* **2019**, *9*, 10245−10252.
(18) de Azambuja, F.; Lenie, J.; Parac-Vogt, T. N. Homogeneous Metal Catalysts with Inorganic Ligands: Probing Ligand Effects in Lewis Acid Catalyzed Direct Amide Bond Formation. *ACS Catal.* **2021**, *11*, 271−277.
(19) Calcio Gaudino, E.; Carnaroglio, D.; Nunes, M. A. G.; Schmidt, L.; Flores, E. M. M.; Deiana, C.; Sakhno, Y.; Martra, G.; Cravotto, G. Fast TiO_2-catalyzed direct amidation of neat carboxylic acids under mild dielectric heating. *Catal. Sci. Technol.* **2014**, *4*, 1395−1399.
(20) Gu, L.; Lim, J.; Cheong, J. L.; Lee, S. S. MCF-supported boronic acids as efficient catalysts for direct amide condensation of carboxylic acids and amines. *Chem. Commun.* **2014**, *50*, 7017−7019.
(21) Ali, M. A.; Siddiki, S. M. A. H.; Onodera, W.; Kon, K.; Shimizu, K.-i. Amidation of Carboxylic Acids with Amines by Nb2O5 as a Reusable Lewis Acid Catalyst. *ChemCatChem* **2015**, *7*, 3555−3561.
(22) Zakharova, M. V.; Kleitz, F.; Fontaine, F.-G. Lewis acidity quantification and catalytic activity of Ti, Zr and Al-supported mesoporous silica. *Dalton Trans.* **2017**, *46*, 3864−3876.
(23) Deiana, C.; Sakhno, Y.; Fabbiani, M.; Pazzi, M.; Vincenti, M.; Martra, G. Direct Synthesis of Amides from Carboxylic Acids and Amines by Using Heterogeneous Catalysts: Evidence of Surface Carboxylates as Activated Electrophilic Species. *ChemCatChem* **2013**, *5*, 2832−2834.
(24) Arena, F.; Deiana, C.; Lombardo, A. F.; Ivanchenko, P.; Sakhno, Y.; Trunfio, G.; Martra, G. Activity patterns of metal oxide catalysts in the synthesis of N-phenylpropionamide from propanoic acid and aniline. *Catal. Sci. Technol.* **2015**, *5*, 1911−1918.
(25) Siddiki, S. M. A. H.; Rashed, M. N.; Ali, M. A.; Toyao, T.; Hirunsit, P.; Ehara, M.; Shimizu, K.-i. Lewis Acid Catalysis of Nb_2O_5 for Reactions of Carboxylic Acid Derivatives in the Presence of Basic Inhibitors. *ChemCatChem* **2019**, *11*, 383−396.
(26) Samantaray, M. K.; Pump, E.; Bendjeriou-Sedjerari, A.; D'Elia, V.; Pelletier, J. D. A.; Guidotti, M.; Psaro, R.; Basset, J.-M. Surface organometallic chemistry in heterogeneous catalysis. *Chem. Soc. Rev.* **2018**, *47*, 8403−8437.
(27) Samantaray, M. K.; D'Elia, V.; Pump, E.; Falivene, L.; Harb, M.; Ould Chikh, S.; Cavallo, L.; Basset, J.-M. The Comparison between Single Atom Catalysis and Surface Organometallic Catalysis. *Chem. Rev.* **2020**, *120*, 734−813.
(28) Corma, A.; García, H.; Llabrés i Xamena, F. X. Engineering Metal Organic Frameworks for Heterogeneous Catalysis. *Chem. Rev.* **2010**, *110*, 4606−4655.
(29) Dhakshinamoorthy, A.; Li, Z.; Garcia, H. Catalysis and photocatalysis by metal organic frameworks. *Chem. Soc. Rev.* **2018**, *47*, 8134−8172.
(30) Pascanu, V.; González Miera, G.; Inge, A. K.; Martín-Matute, B. Metal−Organic Frameworks as Catalysts for Organic Synthesis: A Critical Perspective. *J. Am. Chem. Soc.* **2019**, *141*, 7223−7234.
(31) Yang, D.; Gates, B. C. Catalysis by Metal Organic Frameworks: Perspective and Suggestions for Future Research. *ACS Catal.* **2019**, *9*, 1779−1798.
(32) Bavykina, A.; Kolobov, N.; Khan, I. S.; Bau, J. A.; Ramirez, A.; Gascon, J. Metal−Organic Frameworks in Heterogeneous Catalysis: Recent Progress, New Trends, and Future Perspectives. *Chem. Rev.* **2020**, *120*, 8468−8535.
(33) Diercks, C. S.; Kalmutzki, M. J.; Diercks, N. J.; Yaghi, O. M. Conceptual Advances from Werner Complexes to Metal−Organic Frameworks. *ACS Cent. Sci.* **2018**, *4*, 1457−1464.
(34) Fang, Z.; Bueken, B.; De Vos, D. E.; Fischer, R. A. Defect-Engineered Metal−Organic Frameworks. *Angew. Chem., Int. Ed.* **2015**, *54*, 7234−7254.
(35) DeStefano, M. R.; Islamoglu, T.; Garibay, S. J.; Hupp, J. T.; Farha, O. K. Room-Temperature Synthesis of UiO-66 and Thermal Modulation of Densities of Defect Sites. *Chem. Mater.* **2017**, *29*, 1357−1361.
(36) Feng, X.; Hajek, J.; Jena, H. S.; Wang, G.; Veerapandian, S. K. P.; Morent, R.; De Geyter, N.; Leyssens, K.; Hoffman, A. E. J.; Meynen, V.; Marquez, C.; De Vos, D. E.; Van Speybroeck, V.; Leus, K.; Van Der Voort, P. Engineering a Highly Defective Stable UiO-66 with Tunable Lewis-Brønsted Acidity: The Role of the Hemilabile Linker. *J. Am. Chem. Soc.* **2020**, *142*, 3174−3183.
(37) Todorovic, M.; Perrin, D. M. Recent developments in catalytic amide bond formation. *Pept. Sci.* **2020**, *112*, No. e24210.
(38) Cirujano, F. G.; Corma, A.; Llabrés i Xamena, F. X. Conversion of levulinic acid into chemicals: Synthesis of biomass derived levulinate esters over Zr-containing MOFs. *Chem. Eng. Sci.* **2015**, *124*, 52−60.
(39) Cirujano, F. G.; Corma, A.; Llabrés i Xamena, F. X. Zirconium-containing metal organic frameworks as solid acid catalysts for the esterification of free fatty acids: Synthesis of biodiesel and other compounds of interest. *Catal. Today* **2015**, *257*, 213−220.
(40) Caratelli, C.; Hajek, J.; Cirujano, F. G.; Waroquier, M.; Llabrés i Xamena, F. X.; Van Speybroeck, V. Nature of active sites on UiO-66 and beneficial influence of water in the catalysis of Fischer esterification. *J. Catal.* **2017**, *352*, 401−414.
(41) Wang, F.; Chen, Z.; Chen, H.; Goetjen, T. A.; Li, P.; Wang, X.; Alayoglu, S.; Ma, K.; Chen, Y.; Wang, T.; Islamoglu, T.; Fang, Y.; Snurr, R. Q.; Farha, O. K. Interplay of Lewis and Brønsted Acid Sites in Zr-Based Metal−Organic Frameworks for Efficient Esterification of Biomass-Derived Levulinic Acid. *ACS Appl. Mater. Interfaces* **2019**, *11*, 32090−32096.
(42) Villoria-del-Álamo, B.; Rojas-Buzo, S.; García-García, P.; Corma, A. Zr-MOF-808 as Catalyst for Amide Esterification. *Chem. - Eur. J.* **2021**, *27*, 4588−4598.
(43) Hoang, L. T. M.; Ngo, L. H.; Nguyen, H. L.; Nguyen, H. T. H.; Nguyen, C. K.; Nguyen, B. T.; Ton, Q. T.; Nguyen, H. K. D.; Cordova, K. E.; Truong, T. An azobenzene-containing metal−organic framework as an efficient heterogeneous catalyst for direct amidation of benzoic acids: synthesis of bioactive compounds. *Chem. Commun.* **2015**, *51*, 17132−17135.
(44) Moons, J.; de Azambuja, F.; Mihailovic, J.; Kozma, K.; Smiljanic, K.; Amiri, M.; Cirkovic Velickovic, T.; Nyman, M.; Parac-Vogt, T. N. Discrete Hf_{18} Metal-oxo Cluster as a Heterogeneous Nanozyme for Site-Specific Proteolysis. *Angew. Chem., Int. Ed.* **2020**, *59*, 9094−9101.
(45) de Azambuja, F.; Moons, J.; Parac-Vogt, T. N. The Dawn of Metal-Oxo Clusters as Artificial Proteases: From Discovery to the Present and Beyond. *Acc. Chem. Res.* **2021**, *54*, 1673−1684.
(46) Ly, H. G. T.; Fu, G.; Kondinski, A.; Bueken, B.; De Vos, D.; Parac-Vogt, T. N. Superactivity of MOF-808 toward Peptide Bond Hydrolysis. *J. Am. Chem. Soc.* **2018**, *140*, 6325−6335.
(47) Conic, D.; Pierloot, K.; Parac-Vogt, T. N.; Harvey, J. N. Mechanism of the highly effective peptide bond hydrolysis by MOF-808 catalyst under biologically relevant conditions. *Phys. Chem. Chem. Phys.* **2020**, *22*, 25136−25145.
(48) Loosen, A.; de Azambuja, F.; Smolders, S.; Moons, J.; Simms, C.; De Vos, D.; Parac-Vogt, T. N. Interplay between structural parameters and reactivity of Zr_6-based MOFs as artificial proteases. *Chem. Sci.* **2020**, *11*, 6662−6669.
(49) Ly, H. G. T.; Fu, G.; de Azambuja, F.; De Vos, D. E.; Parac-Vogt, T. N. Nanozymatic Activity of UiO-66 Metal-Organic Frameworks: Tuning the Nanopore Environment Enhances Hydrolytic Activity toward Peptide Bonds. *ACS Appl. Nano Mater.* **2020**, *3*, 8931−8938.
(50) James Cleaves Ii, H.; Michalkova Scott, A.; Hill, F. C.; Leszczynski, J.; Sahai, N.; Hazen, R. Mineral−organic interfacial processes: potential roles in the origins of life. *Chem. Soc. Rev.* **2012**, *41*, 5502−5525.
(51) Kitadai, N.; Nishiuchi, K. Thermodynamic Impact of Mineral Surfaces on Amino Acid Polymerization: Aspartate Dimerization on Goethite. *Astrobiology* **2019**, *19*, 1363−1376.

https://doi.org/10.1021/acscatal.1c01782
ACS Catal. 2021, 11, 7647−7658

(52) Rimola, A.; Sodupe, M.; Ugliengo, P. Role of Mineral Surfaces in Prebiotic Chemical Evolution. In Silico Quantum Mechanical Studies. *Life* **2019**, *9*, 10.
(53) Sakhno, Y.; Battistella, A.; Mezzetti, A.; Jaber, M.; Georgelin, T.; Michot, L.; Lambert, J.-F. One Step up the Ladder of Prebiotic Complexity: Formation of Nonrandom Linear Polypeptides from Binary Systems of Amino Acids on Silica. *Chem. – Eur. J.* **2019**, *25*, 1275−1285.
(54) de Castro Silva, F.; Lima, L. C. B.; Silva-Filho, E. C.; Fonseca, M. G.; Lambert, J.-F.; Jaber, M. A comparative study of alanine adsorption and condensation to peptides in two clay minerals. *Appl. Clay Sci.* **2020**, *192*, No. 105617.
(55) Rimola, A.; Costa, D.; Sodupe, M.; Lambert, J.-F.; Ugliengo, P. Silica Surface Features and Their Role in the Adsorption of Biomolecules: Computational Modeling and Experiments. *Chem. Rev.* **2013**, *113*, 4216−4313.
(56) Martra, G.; Deiana, C.; Sakhno, Y.; Barberis, I.; Fabbiani, M.; Pazzi, M.; Vincenti, M. The Formation and Self-Assembly of Long Prebiotic Oligomers Produced by the Condensation of Unactivated Amino Acids on Oxide Surfaces. *Angew. Chem., Int. Ed.* **2014**, *53*, 4671−4674.
(57) Rimola, A.; Fabbiani, M.; Sodupe, M.; Ugliengo, P.; Martra, G. How Does Silica Catalyze the Amide Bond Formation under Dry Conditions? Role of Specific Surface Silanol Pairs. *ACS Catal.* **2018**, *8*, 4558−4568.
(58) Guo, C.; Jordan, J. S.; Yarger, J. L.; Holland, G. P. Highly Efficient Fumed Silica Nanoparticles for Peptide Bond Formation: Converting Alanine to Alanine Anhydride. *ACS Appl. Mater. Interfaces* **2017**, *9*, 17653−17661.
(59) Howarth, A. J.; Liu, Y.; Li, P.; Li, Z.; Wang, T. C.; Hupp, J. T.; Farha, O. K. Chemical, thermal and mechanical stabilities of metal−organic frameworks. *Nat. Rev. Mater.* **2016**, *1*, 1−15.
(60) Cavka, J. H.; Jakobsen, S.; Olsbye, U.; Guillou, N.; Lamberti, C.; Bordiga, S.; Lillerud, K. P. A new zirconium inorganic building brick forming metal organic frameworks with exceptional stability. *J. Am. Chem. Soc.* **2008**, *130*, 13850−13851.
(61) Rimoldi, M.; Howarth, A. J.; DeStefano, M. R.; Lin, L.; Goswami, S.; Li, P.; Hupp, J. T.; Farha, O. K. Catalytic Zirconium/Hafnium-Based Metal−Organic Frameworks. *ACS Catal.* **2017**, *7*, 997−1014.
(62) Reinsch, H.; Waitschat, S.; Chavan, S. M.; Lillerud, K. P.; Stock, N. A facile "green" route for scalable batch production and continuous synthesis of zirconium MOFs. *Eur. J. Inorg. Chem.* **2016**, *2016*, 4490−4498.
(63) Wang, T. C.; Vermeulen, N. A.; Kim, I. S.; Martinson, A. B.; Stoddart, J. F.; Hupp, J. T.; Farha, O. K. Scalable synthesis and post-modification of a mesoporous metal-organic framework called NU-1000. *Nat. Protoc.* **2016**, *11*, 149−162.
(64) Katz, M. J.; Brown, Z. J.; Colón, Y. J.; Siu, P. W.; Scheidt, K. A.; Snurr, R. Q.; Hupp, J. T.; Farha, O. K. A facile synthesis of UiO-66, UiO-67 and their derivatives. *Chem. Commun.* **2013**, *49*, 9449−9451.
(65) Pan, L.; Heddy, R.; Li, J.; Zheng, C.; Huang, X.-Y.; Tang, X.; Kilpatrick, L. Synthesis and Structural Determination of a Hexanuclear Zirconium Glycine Compound Formed in Aqueous Solution. *Inorg. Chem.* **2008**, *47*, 5537−5539.
(66) Kickelbick, G.; Feth, M. P.; Bertagnolli, H.; Puchberger, M.; Holzinger, D.; Gross, S. Formation of organically surface-modified metal oxo clusters from carboxylic acids and metal alkoxides: a mechanistic study. *J. Chem. Soc., Dalton Trans.* **2002**, 3892−3898.
(67) Liu, X.; Wang, X.; Kapteijn, F. Water and Metal−Organic Frameworks: From Interaction toward Utilization. *Chem. Rev.* **2020**, *120*, 8303−8377.
(68) Kobayashi, S.; Nagayama, S.; Busujima, T. Lewis Acid Catalysts Stable in Water. Correlation between Catalytic Activity in Water and Hydrolysis Constants and Exchange Rate Constants for Substitution of Inner-Sphere Water Ligands. *J. Am. Chem. Soc.* **1998**, *120*, 8287−8288.
(69) Zhang, Y.; de Azambuja, F.; Parac-Vogt, T. N. The forgotten chemistry of group(IV) metals: A survey on the synthesis, structure, and properties of discrete Zr(IV), Hf(IV), and Ti(IV) oxo clusters. *Coord. Chem. Rev.* **2021**, *438*, No. 213886.
(70) Mihaylov, T. T.; Ly, H. G. T.; Pierloot, K.; Parac-Vogt, T. N. Molecular Insight from DFT Computations and Kinetic Measurements into the Steric Factors Influencing Peptide Bond Hydrolysis Catalyzed by a Dimeric Zr(IV)-Substituted Keggin Type Polyoxometalate. *Inorg. Chem.* **2016**, *55*, 9316−9328.
(71) Lundberg, H.; Tinnis, F.; Zhang, J.; Algarra, A. G.; Himo, F.; Adolfsson, H. Mechanistic Elucidation of Zirconium-Catalyzed Direct Amidation. *J. Am. Chem. Soc.* **2017**, *139*, 2286−2295.
(72) Caratelli, C.; Hajek, J.; Rogge, S. M. J.; Vandenbrande, S.; Meijer, E. J.; Waroquier, M.; Van Speybroeck, V. Influence of a Confined Methanol Solvent on the Reactivity of Active Sites in UiO-66. *ChemPhysChem* **2018**, *19*, 420−429.
(73) Tullberg, M.; Grøtli, M.; Luthman, K. Efficient synthesis of 2,5-diketopiperazines using microwave assisted heating. *Tetrahedron* **2006**, *62*, 7484−7491.
(74) Forsythe, J. G.; Yu, S.-S.; Mamajanov, I.; Grover, M. A.; Krishnamurthy, R.; Fernández, F. M.; Hud, N. V. Ester-Mediated Amide Bond Formation Driven by Wet−Dry Cycles: A Possible Path to Polypeptides on the Prebiotic Earth. *Angew. Chem., Int. Ed.* **2015**, *54*, 9871−9875.
(75) Schapp, J.; Beck, W. Metal complexes of biologically important ligands. Part CXLVIII. Synthesis of peptides from glycine ester catalyzed by triflates and chlorides of metal(III, IV and VI) ions. *Z. Naturforsch., B: J. Chem. Sci.* **2003**, *58*, 85−91.
(76) Yang, D.; Bernales, V.; Islamoglu, T.; Farha, O. K.; Hupp, J. T.; Cramer, C. J.; Gagliardi, L.; Gates, B. C. Tuning the Surface Chemistry of Metal Organic Framework Nodes: Proton Topology of the Metal-Oxide-Like Zr_6 Nodes of UiO-66 and NU-1000. *J. Am. Chem. Soc.* **2016**, *138*, 15189−15196.
(77) Yang, D.; Ortuño, M. A.; Bernales, V.; Cramer, C. J.; Gagliardi, L.; Gates, B. C. Structure and Dynamics of Zr_6O_8 Metal−Organic Framework Node Surfaces Probed with Ethanol Dehydration as a Catalytic Test Reaction. *J. Am. Chem. Soc.* **2018**, *140*, 3751−3759.
(78) Mantz, Y. A.; Gerard, H.; Iftimie, R.; Martyna, G. J. Isomerization of a Peptidic Fragment Studied Theoretically in Vacuum and in Explicit Water Solvent at Finite Temperature. *J. Am. Chem. Soc.* **2004**, *126*, 4080−4081.
(79) Mantz, Y. A.; Gerard, H.; Iftimie, R.; Martyna, G. J. Ab Initio and Empirical Model MD Simulation Studies of Solvent Effects on the Properties of N-Methylacetamide along a cis−trans Isomerization Pathway. *J. Phys. Chem. B* **2006**, *110*, 13523−13538.
(80) Mantz, Y. A.; Branduardi, D.; Bussi, G.; Parrinello, M. Ensemble of Transition State Structures for the Cis−Trans Isomerization of N-Methylacetamide. *J. Phys. Chem. B* **2009**, *113*, 12521−12529.
(81) Li, P.; Chen, X. G.; Shulin, E.; Asher, S. A. UV Resonance Raman Ground and Excited State Studies of Amide and Peptide Isomerization Dynamics. *J. Am. Chem. Soc.* **1997**, *119*, 1116−1120.
(82) Xia, P.; Wang, C.; Qi, C. Theoretical Study on the Cyclization Mechanism of Dipeptides. *Chin. J. Chem.* **2013**, *31*, 813−818.
(83) Grommet, A. B.; Feller, M.; Klajn, R. Chemical reactivity under nanoconfinement. *Nat. Nanotechnol.* **2020**, *15*, 256−271.
(84) Charville, H.; Jackson, D.; Hodges, G.; Whiting, A. The thermal and boron-catalysed direct amide formation reactions: mechanistically understudied yet important processes. *Chem. Commun.* **2010**, *46*, 1813−1823.
(85) Yang, D.; Gaggioli, C. A.; Ray, D.; Babucci, M.; Gagliardi, L.; Gates, B. C. Tuning Catalytic Sites on Zr_6O_8 Metal−Organic Framework Nodes via Ligand and Defect Chemistry Probed with tert-Butyl Alcohol Dehydration to Isobutylene. *J. Am. Chem. Soc.* **2020**, *142*, 8044−8056.
(86) Lundberg, H.; Tinnis, F.; Adolfsson, H. Direct Amide Coupling of Non-activated Carboxylic Acids and Amines Catalysed by Zirconium(IV) Chloride. *Chem. – Eur. J.* **2012**, *18*, 3822−3826.
(87) Lundberg, H.; Tinnis, F.; Adolfsson, H. Titanium(IV) Isopropoxide as an Efficient Catalyst for Direct Amidation of Nonactivated Carboxylic Acids. *Synlett* **2012**, *23*, 2201−2204.

https://doi.org/10.1021/acscatal.1c01782
ACS Catal. 2021, 11, 7647−7658

(88) Tinnis, F.; Lundberg, H.; Adolfsson, H. Direct Catalytic Formation of Primary and Tertiary Amides from Non-Activated Carboxylic Acids, Employing Carbamates as Amine Source. *Adv. Synth. Catal.* **2012**, *354*, 2531−2536.

https://doi.org/10.1021/acscatal.1c01782
ACS Catal. 2021, 11, 7647−7658